

IGF-1 loaded injectable microspheres for potential repair of the infarcted myocardium

Elisabetta Rosellini^{1*}, Nicoletta Barbani¹, Caterina Frati², Denise Madeddu², Diana Massai³,
Umberto Morbiducci³, Luigi Lazzeri¹, Angela Falco², Gallia Graiani⁴, Costanza Lagrasta², Alberto
Audenino³, Maria Grazia Cascone¹, Federico Quaini²

¹Department of Civil and Industrial Engineering, University of Pisa, Pisa, Italy

²Department of Medicine and Surgery, University of Parma, Parma, Italy

³Department of Mechanical and Aerospace Engineering, Politecnico di Torino, Torino, Italy

⁴University of Parma Dental Medicine Unit, Parma, Italy

* To whom correspondence should be addressed. Tel.: +39 050 2217908. Fax: +39 050 2217866. E-mail: elisabetta.rosellini@unipi.it

Abstract

The use of injectable scaffolds to repair the infarcted heart is receiving great interest.

Thermosensitive polymers, *in situ* polymerization, *in situ* cross-linking, and self-assembling peptides are the most investigated approaches to obtain injectability.

Aim of the present work was the preparation and characterization of a novel bioactive scaffold, in form of injectable microspheres, for cardiac repair. Gellan/gelatin microspheres were prepared by a water-in-oil emulsion and loaded by adsorption with Insulin-like growth factor 1 to promote tissue regeneration. Obtained microspheres underwent morphological, physicochemical and biological characterization, including cell culture tests in static and dynamic conditions and *in vivo* tests.

Morphological analysis of the microspheres showed a spherical shape, a microporous surface and an average diameter of $66\pm 17\mu\text{m}$ (under dry conditions) and $123\pm 24\mu\text{m}$ (under wet conditions).

Chemical Imaging analysis pointed out a homogeneous distribution of gellan, gelatin and Insulin-like growth factor-1 within the microsphere matrix. *In vitro* cell culture tests showed that the microspheres promoted rat cardiac progenitor cells adhesion, and cluster formation. After dynamic suspension culture within an impeller-free bioreactor, cells still adhered to microspheres, spreading their cytoplasm over microsphere surface. Intramyocardial administration of microspheres in a cryoinjury rat model attenuated chamber dilatation, myocardial damage and fibrosis and improved cell homing.

Overall, the findings of this study confirm that the produced microspheres display morphological, physicochemical, functional and biological properties potentially adequate for future applications as injectable scaffold for cardiac tissue engineering.

Keywords: Insulin-like growth factor 1, gelatin, gellan, functionalization, cardiac tissue engineering

1. Introduction

Cardiac tissue engineering aims to regenerate the diseased myocardium using combinations of cells, scaffolds and signals [1, 2]. In a widely explored approach, cells are cultured *in vitro* on a preformed three-dimensional polymeric scaffold, to obtain a tissue-engineered patch to be implanted on the damaged heart surface [3, 4]. This approach provides a template for structural organization of the cells with good control on construct shape and size, cell sources and retention, and tissue development. However, its translation to clinics is limited by restricted cell expansion and extracellular matrix formation inside the scaffold, by the non-trivial connection with the native vascular network after transplantation with the consequent risk of necrosis, and by functional properties that do not yet match the native myocardium [5]. An alternative to the *in vitro* strategy is the *in vivo* tissue engineering approach, based on the implantation/injection of an unseeded scaffold or injectable biomaterial on the damaged myocardium, designed to create a favourable environment for cell proliferation and differentiation [6]. The *in vivo* approach, aiming at replacing the injured tissue in its natural milieu, could be more effective and easier to manage than the *in vitro* one [6]. A key step for a successful *in vivo* approach is the scaffold biofunctionalization, aimed at promoting endogenous tissue regeneration through the release of bioactive molecules (such as growth factors) to the surrounding cells [7]. Christmas and colleagues were the first to demonstrate that skeletal myoblast delivery to the rat myocardium through an injectable scaffold leads to an improved cell survival, compared to the injection of cells alone (the classical cellular cardiomyoplasty technique) [8].

Natural polymers, including fibrin [8], collagen [9], fibrinogen [10], alginate [11], chitosan [12], solubilized extracellular matrix [13] and Matrigel [14], have been investigated for application as injectable scaffolds for myocardial tissue repair, normally using *in situ* cross-linking and *in situ* polymerization as strategies to obtain injectability. Self-assembling peptides [15] and synthetic thermoreversible polymers [16] have been also proposed.

The development of microspheres-based injectable scaffolds, acting as microcarriers, can represent an effective alternative. It has been already demonstrated that microspheres-based injectable scaffolds support cell culture, they are advantageous for maintaining a differentiated cell phenotype, and their high surface area allows rapid cell expansion [17]. Several factors affect their performance in tissue regeneration applications. In detail, cell attachment to the microsphere surface depends on a plethora of parameters, ranging from the chemical composition to the porosity and hydrophilicity degree. In addition, the number of cells that attach onto the surface of a single microsphere depends upon its diameter. For this reason, microspheres size distribution should be as narrow as possible to provide homogeneous culture conditions.

The use of injectable microspheres for myocardial regeneration has been explored to a very limited extent [18-19]. In a previous study, we reported the preparation of gelatin/gellan (Gel/GE) microparticles and we demonstrated that their physicochemical and functional properties are adequate for tissue engineering application [19]. Moreover, we investigated the effect of their diameter on cardiac progenitor cells (CPCs), showing a preferential CPCs adhesion to microparticles with a smaller size [19]. However, even the smaller particles of our previous study had a swollen diameter above 200 μm . As demonstrated in literature, injectable microspheres for tissue engineering should have a diameter below 200 μm , to allow adequate diffusion of oxygen, nutrients and metabolic products [20]. Moreover, smaller particles offer the advantage of a higher surface to volume ratio, which can permit a higher cell adhesion.

Aim of the present work was the development and characterization of a novel microspheres-based bioactive injectable scaffold for cardiac tissue engineering, combining (i) a narrow size distribution, with an average wet diameter below 200 μm ; (ii) bioactivity, given by the release of a growth factor, promoting heart regeneration.

Microspheres were obtained by a water-in-oil emulsion, using a Gel/GE blend. Phosphatidylcholine (PC), a phospholipid from biological membranes, was used as surfactant. As already demonstrated [19], Gel/GE microspheres present a marked capability to absorb water, which makes them very

similar to soft tissues as the myocardium. Moreover, the hydrogelic nature of the proposed microspheres can favor the controlled release of bioactive agents [21]. In this work, Gel/GE microspheres were functionalized by loading with Insulin-like growth factor 1 (IGF-1), a growth factor able to promote homing, engraftment and differentiation of cardiac progenitor cells, as well as to improve revascularization [22-24]. As reported in literature, IGF-1 (IGF-1) overexpression in cardiomyocytes of transgenic mice prevents cell death as a result of acute myocardial infarction, reducing reactive hypertrophy, ventricular dilatation and wall stress. In addition, IGF-1 overexpression is able to significantly attenuate necrotic and apoptotic death in mice exposed to chronic diffuse ischemic insult. Moreover, the specific overexpression of IGF-1 receptor increases cardiomyocytes formation, reduces apoptotic death and delays cardiomyopathy due to the aging process. In the heart, the IGF-1 receptor system induces cardiac stem cells proliferation, increases telomerase activity, attenuates replicative senescence and preserves the functionally competent pool of stem cells. The IGF-1 loading procedure was optimized in this paper to obtain a sustained release from the microspheres over a few days.

The results of the *in vitro* characterization, including a biological evaluation with CPCs, are illustrated. Additionally, *in vivo* experiments in a small animal model are reported.

2. Material and methods

2.1 Materials

Gel (type B from bovine skin), GE, PC and phosphate buffer solution (PBS) were supplied by Sigma Aldrich (St. Louis, MO, USA).

Dichloromethane, isopropanol and calcium chloride were purchased by Carlo Erba Reagenti (Italy).

Rat IGF-1 was provided by Immunological and Biochemical test systems GMBH (Germany).

Other reagents were all analytical grade, commercially available and used as received.

2.2 Microspheres production

Gel/GE microspheres were prepared by a water-in-oil emulsion, using a procedure adapted from our previous work [19]. Here the preparation procedure was optimized to obtain particles with spherical shape and reduces diameters. The water phase was made by 50 ml of a 2 % (w/v) solution of the two biopolymers (Gel/GE, weight ratio 30/70) in bi-distilled water; the oil phase was 400 ml of a 1.5 % (w/v) solution of PC in dichloromethane.

The oil phase was maintained under constant stirring, at a temperature of 40°C. The water phase was added drop by drop to the oil phase, maintaining the water phase at controlled temperature (40°C) during drip.

The emulsion comprised three steps: 30 mins at 40°C, under stirring at 800 rpm; 1 hr at room temperature, under stirring at 800 rpm; 2 hr at 0°C, under stirring at 500 rpm.

At the end of the emulsion phase, the reaction mixture was collected in a separating funnel for decantation. Microspheres were separated from the oil phase and repeatedly washed with isopropanol to remove PC. Then, they were immersed for 15 mins in a 2% (w/v) CaCl₂ solution in bi-distilled water for GE cross-linking.

Microspheres removed from the cross-linking bath were collected on filter paper and dried under hood overnight.

2.3 Microspheres functionalization

Microspheres functionalization was performed by loading with IGF-1. As the water in oil emulsion could denature the growth factor, IGF-1 was loaded by adsorption on preformed microspheres, using 0.25 µg IGF-1/mg microspheres. Two different loading strategies were tested. In the first one (method A), a fixed amount of microspheres, already cross-linked with calcium ions, was maintained in contact with a solution of IGF-1, until complete adsorption. Alternatively, a fixed amount of uncross-linked microspheres was put in contact with a solution of IGF-1 in bi-distilled water containing also calcium ions (2% w/v of CaCl₂), until complete adsorption (method B).

Based on microspheres swelling behavior knowledge [19], a volume of IGF-1 solution adequate to achieve full adsorption was used in both methods (A and B).

2.4 Morphological analysis

A scanning electron microscope (SEM JSM 5600, Jeol Ltd, Tokyo, Japan) was used to investigate the morphology of the produced microspheres.

Before analysis, dried samples were sprayed with a 200-500 Å gold layer.

An optical microscope (integrated with the Spotlight 400 FT IR Imaging System, Perkin Elmer, Waltham, MA, USA) was used to measure microspheres average wet diameter, as the particles will be in a swollen state during both *in vitro* cell culture and *in vivo* injection. A sample of $N > 100$ microspheres was immersed in PBS for 15 mins and then observed at the microscope.

2.5 Infrared analysis

Infrared analysis was applied (1) to study the chemical composition and chemical homogeneity of the microspheres, (2) to verify the presence and the distribution of the bioactive agent within the microsphere matrix and (3) to characterize the explants of *in vivo* tests, investigating possible alterations of protein conformation in the treated myocardial tissue.

2.5.1 Attenuated total reflectance (ATR) Fourier transformed infrared (FT-IR) spectroscopy analysis

Infrared spectra of the samples were obtained with a FT-IR Spectrometer (Perkin Elmer Spectrum One FT-IR Spectrometer), equipped with ATR objective lens with a penetration depth of less than 1 μm . All spectra were obtained at 4 cm^{-1} , representing the average of 16 scans.

2.5.2 Infrared Chemical Imaging

Spectral images were acquired in transmission mode using an infrared imaging system (Spotlight 300, Perkin Elmer) in the range $4000\text{-}600\text{ cm}^{-1}$. The spectral resolution was 4 cm^{-1} . The spatial resolution was $6\text{ }\mu\text{m}$. Samples were positioned on a BaF_2 support before analysis.

Spectral image processing was performed applying the Spotlight software. In particular, in order to investigate the distribution of specific components, the presence of diagnostic peaks was verified in the spectra acquired from different points of the chemical map. Alternatively, chemical maps in function of a diagnostic peak were elaborated. Second derivative spectra were also acquired.

2.5.3 Samples preparation for infrared analysis

In order to verify the presence and the distribution of IGF-1 within the microsphere matrix, a small amount of hydrated IGF-1 loaded particles was slightly pressed between two supports made of BaF₂, which is an insoluble salt, transparent to infrared radiation. After the separation of the two supports, microspheres, which remained adherent to support surface, were dried in a ventilated oven and analyzed directly on the BaF₂ support. In this way, it was possible to reduce the thickness of the microspheres to analyze them in transmission mode, which is a more sensitive method, capable of providing spectra related to even very small quantities of material.

For what concerns the infrared analysis of the explants of *in vivo* tests, tissue samples were collected from the injection site, 10 days after injection. Tissue samples were frozen in liquid nitrogen after washing, transported in dry ice and analysed within 24 hours from collection. Before analysis, samples were dried by freeze-drying. The infrared analysis was performed in μ ATR mode.

2.6 IGF-1 release test

In vitro IGF-1 release test was carried out in PBS (pH 7.4) at 37°C under mild stirring. A weighted amount of loaded microspheres was added to a fixed volume of release medium inside a polypropylene vial. At fixed time points (0.5 h, 3 h, 6 h, 24 h, 48 h, 72 h, 144 h), the release medium was completely removed and replaced with an equal volume of fresh PBS. The bioactive molecule released in the medium was quantified using a QuantiProBCA assay kit (Sigma Aldrich, St. Louis, MO, USA). In particular, the amount of IGF-1 released from the microspheres was estimated measuring spectrophotometrically the optical density of the eluates at $\lambda = 562$ nm, against a calibration curve, using bovine serum albumin as per the manufacturer's protocol. The total

amount of bioactive molecule released from the microspheres was calculated by adding the amounts released at different times along the whole interval of observation.

As BCA assay kit measures total amount of released proteins, microspheres without IGF-1 were used as control. These particles were prepared following all the same steps of the loaded microspheres, with the only exception of the absence of the growth factor in the cross-linking solution. At each time point, the release from unloaded microspheres was subtracted to the release from IGF-1 loaded microspheres. In this way, gelatin release was subtracted to get only the release of IGF-1.

2.7 Rat CPCs isolation and culture

CPCs were isolated from Green Fluorescence Protein (GFP^{POS}) transgenic rats (n=3) [25] and cultured as previously described [24, 26]. CPCs at passage 3 and 4 (P3-P4) were employed for the experiments carried on in this study.

2.8 In vitro studies

In vitro studies in static and dynamic suspension conditions were performed. Gel/GE microspheres were sterilized by Ultraviolet light irradiation (UV) and suspended in culture medium (0.06 mg of microspheres/ μ l of culture medium) for 15 min, to obtain microsphere swelling, before cell seeding. IGF-1 functionalized Gel/GE microspheres suspended with GFP^{POS} CPCs in culture medium were observed by an inverted and fluorescence microscope to assess cell-microsphere suspension before starting tests.

2.8.1 Cell culture tests in static conditions

CPCs isolated from GFP^{POS} rat hearts were suspended in culture medium together with IGF-1 functionalized Gel/GE microspheres and seeded at the density of 1.5×10^5 cells/ml.

Cell/microsphere adhesion in static condition was evaluated after 48 hours under an inverted and fluorescence microscope (Leica DMI6000B).

2.8.2 Cell culture tests in dynamic suspension conditions

In vitro cell culture tests in dynamic suspension conditions were performed within an impeller-free bioreactor according to an experimental protocol previously described [19]. The bioreactor was designed to assure cell/microspheres three-dimensional dynamic suspension within a low-shear environment at a slow laminar mixing flow regime. Impellers and/or rotational components, that could induce detrimental forces on CPCs, are avoided. Exhaustive technical details on the bioreactor system have been presented elsewhere [27].

Briefly, CPCs were seeded on microspheres in static condition to promote cell/microspheres adhesion. Cell-seeded microspheres were then cultured within the bioreactor in complete growth medium for 24h.

After dynamic suspension, cultured cells were rescued from the bioreactor vessel, re-suspended in fresh growth medium, seeded in a 96 well plate and analyzed by phase contrast and fluorescence microscopy. The microscopic analysis was repeated after 5 days of static culture in order to verify cell adhesion and survival.

Controls were represented by cells cultured in dynamic suspension in the absence of microspheres (GFP^{POS} CPCs CTRL).

2.9 *In vivo* tests

The effectiveness of Gel/GE microspheres in cardiac repair and regeneration applications was investigated *in vivo* using a cryoinjury rat model. In particular, injectability, detectability and biocompatibility were evaluated.

The study population consisted of male Wistar rats (*Rattus norvegicus*, Charles River, Italy) bred at the University of Parma departmental animal facility, weighing 230-280 g (BW).

The investigation was approved by the Veterinary Animal Care and Use Committee of the University of Parma and conformed with the National Ethical Guidelines (Italian Ministry of Health; D.L.vo 116, January 27, 1992) and the Guide for the Care and Use of Laboratory Animals

(NIH publication no. 85–23, revised 1996). In line with the EU Directive 2010/63/EU recommending limitations in animal use, the minimum of three rats was adopted for the present work.

In vivo studies were performed employing Gel/GE microspheres, functionalized with IGF-1 (Gel/GE +IGF-1), in CPC-seeded (Gel/GE +IGF-1+CPCs, n=4) or unseeded (Gel/GE +IGF-1, n=4) configuration. IGF-1 was selected because its administration is known to increase the capability of injected and resident CPCs to generate functionally competent myocardium within the damaged heart [28].

Two additional groups of rats were injected with Gel/GE microspheres without functionalization in the CPC-seeded (Gel/GE+CPCs, n=4) or unseeded (Gel/GE, n=4) configuration.

Control groups (CTRL) were represented by animals subjected to myocardial damage and injected with 100µl of PBS.

2.9.1 Surgical procedure

The surgical procedure and the subsequent macroscopic examination of the rat myocardium were performed as detailed in previous studies [22, 23, 28]. Briefly, rats were anesthetized with a combination of ketamine (40 mg/kg, i.p, Imalgene, Merial, Milano, Italy) and Medetomidine Hydrochloride (0.15 mg/kg i.p., Domitor, Pfizer Italia S.r.l., Latina, Italy), and artificially ventilated (tidal volume: 8–9 µl/g; stroke rate: 165/min).

An incision was made at the left fourth intercostal space and cryoinjury was induced by punching the epicardium with a 20-gauge copper needle freshly immersed in liquid nitrogen.

Gel/GE microspheres with or without functionalization (3 injections of 30 µl each, containing 0.1 mg of microspheres/µl) were injected in the peri-damaged area. In the seeded configuration, 3×10^5 GFP^{POS} CPCs were added to 100µl of Gel/GE microspheres just before intramyocardial injection.

Sacrifice was performed at 4 and 10 days after cryoinjury. The heart of anesthetized rats was arrested in diastole by injection of 5 ml of cadmium chloride (100 mmol/l iv) and briefly perfused at

physiological mean arterial blood pressure with heparinized PBS, followed by perfusion with 10% of formalin solution. Body weight was recorded.

2.9.2 Cardiac Anatomy

The heart was excised and fixed for 24 h in 10% formalin, and the right ventricle (RV) and the left ventricle (LV), including the septum, were separately weighted. The LV long axis was measured from the aortic valve to the apex with a stereomicroscope (2Biological Instruments). Subsequently, the LV was sliced in three transverse sections corresponding respectively to the base, equatorial portion, and apex. On the equatorial section, LV wall thickness and chamber diameter were measured using the image analysis software Image Pro-plus 4.0 (Media Cybernetics, USA). LV chamber volume was calculated according to the Dodge equation, which equalizes the ventricular cavity to an ellipsoid [29]. Finally, the basal, equatorial, and apical slices were embedded in paraffin, and 5- μ m-thick sections were cut for morphometric and immunohistochemical studies.

2.9.3 Immunohistochemical analysis

Homing of injected GFP^{pos} CPCs suspended in Gel/GE microspheres was determined by immunohistochemistry.

GFP was detected by immunofluorescence. For this purpose, LV sections from different experimental groups were incubated with primary antibody (polyclonal goat anti-GFP, dilution 1:100, Abcam, UK). FITC-conjugated specific secondary antibody was used to detect the epitope. Nuclei were recognized by the blue fluorescence of DAPI (4',6-diamindine-2-phenyndole, Sigma) staining.

In order to evaluate the efficiency of injectable scaffolds to improve GFP^{pos} CPC homing within the damaged myocardium, immunostained sections were analyzed under a fluorescence microscope (Leica DMI6000B). From each experimental animal, photomicrographs were taken from the entire damaged myocardium and the area occupied by GFP^{pos} CPCs signals and their intensity, expressed as Integrated Optical density (IOD), were then evaluated by computer assisted image analysis (Image Pro Plus).

2.10 Data management and statistics

The SPSS statistical package (SPSS, Chicago, IL, USA) was used for the statistical analysis.

Statistics of variables included mean \pm standard error (S.E.M.), paired Student t-test, one-way analysis of variance (post-hoc analyses: Tukey test or Holm-Sidak test, when appropriate).

Statistical significance was set at $p < 0.05$, $p < 0.01$ and $p < 0.001$.

3. Results and discussion

3.1 Morphological analysis

SEM micrographs were acquired before and after microspheres functionalization. All microspheres presented spherical shape and porous surface (figures 1a-b). No significant morphological variation was observed for IGF-1 loaded particles, independently of the loading method (figures 1c-f).

An average diameter of $66 \pm 17 \mu\text{m}$ was measured for dried particles. The average wet diameter, evaluated by observing swollen particles under an optical microscope, was equal to $123 \pm 24 \mu\text{m}$.

These dimensions are suitable for injection through a narrow needle, as it has been shown that polymeric microspheres with a similar diameter are injectable through a 27G needle [30].

Moreover, being the swollen diameter below $200 \mu\text{m}$, this should enhance nutrient and waste exchange maintaining high cell viability [20].

The histograms showing microparticles size dispersion are collected in figure 1 g-h. The polydispersity index, calculated as the percentage ratio between standard deviation and average diameter, was 25.7% for dry particles and 19.5% for wet particles, showing a narrow size distribution.

3.2 Infrared analysis

Results of Chemical Imaging investigation on unloaded microspheres are collected in figures 2a-b.

The chemical map (figure 2a) presented a decrease of absorption, moving from the core of the

microsphere to the surface, demonstrating the solid structure of the microspheres. Spectra acquired from different regions of the chemical map showed the presence of the typical absorption peak of Gel, at 1550 cm^{-1} (Amide II). In order to investigate the distribution of the protein in the microspheres, the chemical map in function of amide II absorption peak was acquired (figure 2b): the decrease of absorption moving from the inner core of the microspheres to the surface showed that the protein was present in greater amounts in the core of the microspheres than on the surface. These results demonstrated that Gel was present in the whole microsphere volume, even if not homogeneously distributed, and its presence could have a positive effect on cell attachment [31]. In fact, Gel distributed on the surface layer of the microspheres could exert a positive effect on cell adhesion as soon as the cells come in contact with the scaffold, while Gel in the core of the microspheres, being not cross-linked, progressively diffuses out of the scaffold and it could guarantee a prolonged beneficial effect on cell response.

Chemical Imaging analysis was repeated after microspheres loading with IGF-1 and results are reported in figure 2c-f.

Preliminarily, IGF-1 spectrum was acquired and compared with that of Gel. The two proteins showed a different absorption band due to Amide II: at 1550 cm^{-1} for Gel; at 1525 cm^{-1} for IGF-1. For both microspheres samples (loaded by methods A and loaded by method B), the maps in function of the Amide II absorption band of IGF-1 (at 1525 cm^{-1}) were elaborated (figures 2c and 2e). From these maps, second derivative spectra in the $1580\text{-}1500\text{ cm}^{-1}$ range were acquired both in the inner core of the microspheres and on the surface (figures 2d and 2f).

As shown in figure 2d, for microspheres loaded by method A, Gel absorption peak (at 1550 cm^{-1}) was evident in both spectra, while IGF-1 absorption peak (at 1525 cm^{-1}) was detectable only in the spectrum acquired on the surface of the microspheres. On the opposite, for microspheres loaded by method B (figure 2f), IGF-1 absorption peak was evident also in the core. The obtained results suggest that when microspheres are loaded and cross-linked at the same time (method B), the growth factor is entrapped not only onto the surface but also within the microsphere matrix. The

presence of the bioactive agent within the entire microsphere volume is advantageous, as it could allow a more prolonged release over time.

3.3 IGF-1 release test

IGF-1 was loaded in the produced microspheres by adsorption. Polymeric microspheres are typical monolithic systems for the release of bioactive agents. As reported in literature, in monolithic systems the bioactive agent is dissolved or dispersed within a polymer matrix and the diffusion of the agent through the polymeric matrix allows its release [32]. However, when a biomolecule is loaded by adsorption, the release is generally very quick [33]. Therefore, we tested two loading methods: in method A, loading was performed on cross-linked particles; in method B, loading and cross-linking were performed at the same time. The hypothesis was that method B, producing a cross-linking network around the entrapped molecule, should prolong the release duration.

Release kinetics are collected in figure 3. The obtained results show that the loaded growth factor was completely released during the test, for both methods A and B. However, the release duration was strongly influenced by the loading method. The growth factor loaded by method A was completely released during the first 30 minutes. The obtained quick release could be explained by IGF-1 loading only into a thin surface layer of the microspheres, as already highlighted by infrared analysis.

In the case of loading by method B, a burst release was observed during the first 6 hours (40.4% of IGF-1 released), followed by a slower release, completed in 6 days. The higher initial release rate could be explained by the loss of IGF-1 adsorbed onto microsphere surface. The following lower, gradual release could be attributed to the diffusion of inner IGF-1 out of the microspheres. This diffusion process could be also promoted by the initial degradation of the microsphere matrix. This hypothesis on the mechanism of IGF-1 release is supported by the Chemical Imaging analysis (figure 2), where the presence of growth factor not only on the surface but also in the internal matrix was demonstrated for microspheres loaded by method B.

As reported in literature, a prolonged release of IGF-1 is advantageous for the treatment of infarcted myocardium [34]. Therefore, on the basis of the obtained results, method B was selected for the preparation of IGF-1 functionalized Gel/GE microspheres, intended for cell culture and *in vivo* tests.

The retention of IGF-1 bioactivity after loading in preformed microspheres was not directly verified in this work, as the preservation of IGF-1 activity is already reported in literature for loading procedures that are even less mild than that used in this paper (e.g. working at temperatures up to 60°C and in the presence of organic solvents, while here IGF-1 was dissolved in bi-distilled water and loaded on preformed microspheres at room temperature) [35]. However, the retention of growth factor activity was indirectly verified, through the effect of loaded particles on cell response (both *in vitro* and *in vivo*), as it will be detailed in the next paragraphs.

3.4 *In vitro* studies

3.4.1 *Cell culture tests in static conditions*

The *in vitro* evaluation in static conditions was performed 48 hours after cell seeding. Microscopic observation documented that GFP^{POS} CPCs adhered to the surface of microspheres mainly as individual cells and at time laying their cytoplasm over microsphere surface (figure 4). These results suggest that Gel/GE injectable microspheres allow cell adhesion.

3.4.2 *Cell culture tests in dynamic suspension conditions*

GFP^{POS} CPCs seeded on IGF-1 functionalized Gel/GE microspheres were cultured for 24h in dynamic suspension within the bioreactor. CPCs rescued from the bioreactor vessel still adhered to microspheres (figure 5a), and were occasionally found at the interface between two or more microspheres, resembling connecting elements (figure 5b).

After their collection from the bioreactor, GFP^{POS} CPCs conjugated to Gel/GE microspheres were cultured for 5 days in static conditions. Fluorescence microscopy analysis confirmed that GFP^{POS} CPCs were still adherent to Gel/GE microspheres functionalized with IGF-1. Cells did not display a

round shape and were spreading their cytoplasm over the microsphere surface. Moreover, the presence of both cell-microsphere and cell-cell adhesion was observed (figure 5c-f).

GFP^{pos} CPCs cultured for 5 days after dynamic suspension, were mainly associated to microspheres although individual cells also adhered to the dish. This finding suggests the presence of a strong conjugation between single cells and microspheres, likely attributable to IGF-1 functionalization (figure 5c-f).

3.5 *In vivo tests*

The surgical mortality rate averaged less than 1% in cryoinjured groups at both time points.

3.5.1 *Cardiac Anatomy*

The injection of Gel/GE microspheres did not markedly affect body and cardiac weights at 4 and 10 days (data not shown).

Increased Left Ventricular (LV) chamber volume was documented in CTRL cryoinjured hearts at 10 days when compared to 4 days time point. Intramyocardial injection of unseeded Gel/GE microspheres attenuated LV dilatation both at 4 and 10 days, although microsphere functionalization by IGF-1 did not result in an additive effect on this parameter. However, microspheres seeded with CPCs more effectively reduced LV dilatation, since at day 10 from the surgical procedure, a 2.12-fold decrease in chamber volume was measured compared to CTRL (Table 1).

	Chamber Volume, mm³ (Mean ± St.Dev.)	
	4 Days	10 Days
CTRL	360.01 ± 32.85	410.69 ± 16.88
Gel/GE	172.32 ± 33.16	253.06 ± 44.05

Gel/GE + IGF-1	192.85 ± 70.19	270.75 ± 87.51
Gel/GE + CPCs	196.15 ± 30.62	193.59 ± 1.18 (*)
Gel/GE + IGF-1 + CPCs	153.08 ± 44.61	319.56 ± 13.97

Table 1. Changes in Left Ventricular (LV) chamber volume after cryoinjury in different experimental groups (CTRL: PBS; Gel/GE: Gelatin/Gellan microspheres; IGF-1: Insulin-like Growth Factor-1; CPCs: Cardiac Progenitor Cells). * $p < 0.05$ vs CTRL 10 Days.

3.5.2 Immunohistochemical analysis

The fraction of GFP^{pos} CPCs within the myocardium at day 4 and day 10 from injection, was considered as a measure of homing efficiency. As illustrated in figure 6 injected progenitor cells persisted within the myocardium, although, independently on their association with biomaterials, a time dependent decline was documented. This reduction is likely due to the kinetic of tissue damage, that causes a fast tissue response hampering cell retention. Importantly, functionalization with IGF-1 increased by 4.8-fold at 4 days and by 5-fold at 10 days the number of Gel/GE seeded CPCs in the myocardium (figure 6b).

3.6 Infrared analysis of explants

Explants of rat myocardium, collected at day 10 from microspheres injection (experimental group: Gel/GE + IGF-1 + CPCs), were characterized by means of infrared chemical imaging analysis. The same characterization was carried out, for comparison, on samples of a rat myocardium that was not subjected to myocardial damage, neither was injected with microspheres. As reported in literature, infrared analysis can be used to investigate the chemical composition of cardiac tissue [36]. Results are collected in figure 7.

The medium spectrum from the chemical map of native rat myocardium showed the following typical absorption peaks: Amide A absorption band at 3281 cm^{-1} ; the band due to membrane phospholipid at 1736 cm^{-1} ; Amide I absorption band at 1628 cm^{-1} ; Amide II absorption band at 1524 cm^{-1} ; the band due to polysaccharide components at 1042 cm^{-1} (figure 7a).

Infrared spectra of the explant sample from myocardial damage rat model presented the typical absorption band due to piranosidic ring of GE at 1030 cm^{-1} , thus demonstrating the presence of the microspheres at the injection site. Moreover, an absorption band at 1731 cm^{-1} due to membrane phospholipid was detectable, demonstrating a good presence of cells at the injection site (figure 7c).

Second derivative maps of native myocardial tissue and explants were also acquired to investigate protein secondary structure (figures 7b and 7d). It is well known that the deconvolution of Amide I band is relevant to investigate the conformation of protein material [37, 38]. Second derivative spectrum of native myocardial tissue (figure 7b) was characterized by the following absorption bands: at 1740 cm^{-1} , due to C=O stretching of phospholipids; at 1722 cm^{-1} , due to C=O of nucleic acids; at 1665 cm^{-1} , due to β -turn; at 1656 cm^{-1} , due to α -elix, with a shoulder at 1638 cm^{-1} , due to triple elix; at 1623 cm^{-1} , due to β -sheets structures. The last absorption band due to β -sheet conformation was particularly evident. In the second derivative spectrum of explant sample from myocardial damage rat model (figure 7d), absorption bands at 1740 and 1722 cm^{-1} , due to the presence of cells, were observed, confirming a good CPC homing at 10 days after injection.

Absorption bands at 1655 cm^{-1} , due to α -elix and at 1632 cm^{-1} , due to β -sheets structures, were also detected. Furthermore, the absorption band at 1670 cm^{-1} , due to 3_1 elix, was observed [38]. The 3_1 elix is a β structure, that is present in the terminal telopeptides of tropocollagen molecules.

Therefore, the presence of the relative absorption band is indicative of collagen biosynthesis. In addition, the presence of an intense band at 1648 cm^{-1} was indicative of the presence of collagen involved in the formation of hydrogen bonds, a typical behaviour of less structured collagen, such as the newly synthesised one [38]. Overall, obtained results suggested the deposition of new collagen in the infarcted heart treated with microspheres [36-38].

4. Conclusions

In recent years, injectable scaffolds are receiving a great interest in the field of cardiac tissue engineering. The aim of this work was the preparation and characterization of an innovative bioactive injectable scaffold for infarcted myocardial repair, in the form of IGF-1 loaded microspheres. Microspheres based on a blend of two natural polymers were prepared by a water-in-oil emulsion. Loading with IGF-1 was then performed on preformed microspheres by contact adsorption. IGF-1 was chosen for microspheres functionalization to promote cardiac tissue regeneration.

The obtained microspheres underwent morphological, physicochemical and functional characterization. The morphological analysis showed spherical shape and an average wet diameter of 123 ± 24 μm , that is an adequate dimension for injection through a narrow needle (27G), as well as to promote cell viability. A homogeneous distribution of Gel, GE and IGF-1 within the microsphere matrix was pointed out by infrared Chemical Imaging analysis. The homogeneous distribution of IGF-1, not only on microspheres surface but also in all microspheres volume, has a positive effect on the duration of IGF-1 release. The IGF-1 loading method was in fact optimized by performing at the same time loading and cross-linking, to obtain IGF-1 loading within all microsphere matrix and consequently a gradual release over 6 days. For what concerns the homogeneous distribution of Gel and GE in microspheres polymeric matrix, the advantage is to avoid the presence of regions with different characteristics, to have a homogenous effect on cell response. Moreover, the homogeneous distribution of the different components is a property of native cardiac tissue, as reported in literature [39].

To assess the biocompatibility of the microspheres, cell culture tests were performed both in static and dynamic suspension conditions. For this purpose, GFP^{POS} CPCs were isolated from rat heart and employed as one of the best candidate for myocardial regeneration. A good cell-to-microsphere adhesion was observed, both in static and under dynamic suspension culture and mainly attributable

to IGF-1 functionalization. Interestingly, CPCs were found not only conjugated as single cells but, at times, at the interface between two or more microspheres, resembling connecting elements. *In vivo* tests performed on the cryoinjury rat model confirmed that Gel/GE microspheres were characterized by good injectability. Moreover, Gel/GE microspheres functionalized with IGF-1 improved CPC homing within the host myocardium *in vivo*. Results of the immunohistochemical analysis of the explants were complemented with infrared analysis of the infarcted heart treated with microspheres. This last analysis demonstrated two significant results: a good presence of cells on the infarcted myocardium and the deposition of new collagen.

Overall, Gel/GE microspheres functionalized with IGF-1 have suitable characteristics to be employed as scaffolds for progenitor cells in myocardial regeneration. As future developments toward this goal, further biological investigation will be carried out to confirm the potential clinical implications of these preliminary but encouraging findings. In addition, a next step will be the production of monodisperse bioactive microspheres, using innovative microfluidic devices.

5. Acknowledgments: This work was supported by the European Commission FP7 Programme, grant 214539.

6. References

- [1] Parsa H, Ronaldson K, Vunjak-Novakovic G. Bioengineering methods for myocardial regeneration. *Adv Drug Deliv Rev* 2016; 96: 195-202.
- [2] Ogle BM, Bursac N, Domian I, et al. Distilling complexity to advance cardiac tissue engineering. *Sci Transl Med* 2016; 8: 342ps13.
- [3] Engelmayer GC Jr, Cheng M, Bettinger CJ, et al. Accordion-like honeycombs for tissue engineering of cardiac anisotropy. *Nat Mater* 2008; 7: 1003-1010.
- [4] Rai R, Tallawi M, Barbani N, et al. Biomimetic poly(glycerol sebacate) (PGS) membranes for cardiac patch application. *Mater Sci Eng C Mater Biol Appl* 2013; 33:3677-3687.
- [5] Fujita B, Zimmermann WH. Myocardial Tissue Engineering for Regenerative Applications. *Curr Cardiol Rep* 2017; 19: 78.
- [6] Leor J, Amsalem Y and Cohen S. Cells, scaffolds, and molecules for myocardial tissue engineering. *Pharmacol Therapeut* 2005; 105: 151-163.
- [7] Kretlow JD, Klouda L, Mikos AG. Injectable matrices and scaffolds for drug delivery in tissue engineering. *Adv Drug Deliver Rev* 2007; 59: 263-273.
- [8] Christman KL, Vardanian AJ, Fang Q, et al. Injectable fibrin scaffold improves cell transplant survival, reduces infarct expansion and induces neovasculature formation in ischemic myocardium. *J Am Coll Cardiol* 2004; 44: 654-660.
- [9] Suuronen EJ, Veinot JP, Wong S, et al. Tissue-engineered injectable collagen-based matrices for improved cell delivery and vascularization of ischemic tissue using CD133+ progenitors expanded from the peripheral blood. *Circulation* 2006; 114: I138-I144.
- [10] Shapira-Schweitzer K, Habib M, Gepstein L, et al. A photopolymerizable hydrogel for 3-D culture of human embryonic stem cell-derived cardiomyocytes and rat neonatal cardiac cells. *J Mol Cell Cardiol* 2009; 46: 213-224.
- [11] Landa N, Miller L, Feinberg MS, et al. Effect of injectable alginate implant on cardiac remodeling and function after recent and old infarcts in rat. *Circulation* 2008; 117: 1388-1396.

- [12] Wang H, Shi J, Wang Y, et al. Promotion of cardiac differentiation of brown adipose derived stem cells by chitosan hydrogel for repair after myocardial infarction. *Biomaterials* 2014; 35: 3986-3998.
- [13] Singelyn JM, DeQuach JA, Seif-Naraghi SB, et al. Naturally derived myocardial matrix as an injectable scaffold for cardiac tissue engineering. *Biomaterials* 2009; 30: 5409-5416.
- [14] Kofidis T, Lebl DR, Martinez EC, et al. Novel injectable bioartificial tissue facilitates targeted, less invasive, large-scale tissue restoration on the beating heart after myocardial injury. *Circulation* 2005; 112: Suppl:I173-I177.
- [15] Davis ME, Motion JP, Narmoneva DA, et al. Injectable self-assembling peptide nanofibers create intramyocardial microenvironments for endothelial cells. *Circulation* 2005; 111: 442-450.
- [16] Fujimoto KL, Ma Z, Nelson DM, et al. Synthesis, characterization and therapeutic efficacy of a biodegradable, thermoresponsive hydrogel designed for application in chronic infarcted myocardium. *Biomaterials* 2009; 30: 4357-4368.
- [17] Chen R, Curran SJ, Curran JM, et al. The use of poly(l-lactide) and RGD modified microspheres as cell carriers in a flow intermittency bioreactor for tissue engineering cartilage. *Biomaterials* 2006; 27: 4453-4460.
- [18] Iwakura A, Fujita M, Kataoka K, et al. Intramyocardial sustained delivery of basic fibroblast growth factor improves angiogenesis and ventricular function in a rat infarct model. *Heart Vessels* 2003;18: 93-99.
- [19] Rosellini E, Barbani N, Frati C, et al. Influence of injectable microparticle size on cardiac progenitor cell response. *J Appl Funct Mater* 2018; 16: 241-251.
- [20] McGuigan AP, Sefton MV. Design and Fabrication of Sub-mm-Sized Modules Containing Encapsulated Cells for Modular Tissue Engineering. *Tissue Eng* 2007; 13: 1069-1078.
- [21] Tallawi M, Rosellini E, Barbani N, et al. Strategies for the chemical and biological functionalization of scaffolds for cardiac tissue engineering: a review. *J R Soc Interface* 2015; 12: 20150254.

- [22] Rossini A, Frati C, Lagrasta C, et al. Human cardiac and bone marrow stromal cells exhibit distinctive properties related to their origin. *Cardiovasc Res* 2011; 89: 650-660.
- [23] Bocchi L, Savi M, Graiani G, et al. Growth Factor-Induced Mobilization of Cardiac Progenitor Cells Reduces the Risk of Arrhythmias, in a Rat Model of Chronic Myocardial Infarction. *PLoS One* 2011; 6: e17750.
- [24] Frati C, Savi M, Graiani G, et al. Resident cardiac stem cells. *Curr Pharm Des* 2011; 17 : 3252-3257.
- [25] Okabe M, Ikawa M, Kominami K, et al. 'Green mice' as a source of ubiquitous green cells. *FEBS Lett* 1997; 407: 313-319.
- [26] Giuliani A, Frati C, Rossini A, et al. High-resolution X-ray microtomography for three-dimensional imaging of cardiac progenitor cell homing in infarcted rat hearts. *J Tissue Eng Regen Med* 2011; 5: e168-e178.
- [27] Massai D, Isu G, Madeddu D, et al. A Versatile Bioreactor for Dynamic Suspension Cell Culture. Application to the Culture of Cancer Cell Spheroids. *PLoS One* 2016; 11: e0154610.
- [28] Savi M, Bocchi L, Rossi S, et al. Antiarrhythmic effect of growth factor-supplemented cardiac progenitor cells in chronic infarcted heart. *Am J Physiol Heart Circ Physiol* 2016; 310: H1622-H1648.
- [29] Dodge HT, Baxley WA. Left ventricular volume and mass and their significance in heart disease. *Am J Cardiol* 1969; 23: 528-537.
- [30] Yu J, Du KT, Fang Q, et al. The use of human mesenchymal stem cells encapsulated in RGD modified alginate microspheres in the repair of myocardial infarction in the rat. *Biomaterials* 2010; 31: 7012-7020.
- [31] Wang C, Gong Y, Lin Y, et al. A novel gellan gel-based microcarrier for anchorage-dependent cell delivery. *Acta Biomater* 2008; 4: 1226-1234.
- [32] Brannon-Peppas L. Polymers in controlled drug delivery. *Med Plast Biomater* 1997; 4: 34-44.

- [33] Stulzer HK, Lacerda L, Tagliari MP, et al. Synthesis and characterization of cross-linked malonyl chitosan microspheres for controlled release of acyclovir. *Carbohydr Polym* 2008; 73: 490-497.
- [34] Davis ME, Hsieh PCH, Takahashi T, et al. Local myocardial insulin-like growth factor 1 (IGF-1) delivery with biotinylated peptide nanofibers improves cell therapy for myocardial infarction. *Proc Natl Acad Sci USA* 2006; 103: 8155-8160.
- [35] Clark A, Milbrandt TA, Hilt JZ and Puleo DA. Retention of insulin-like growth factor I bioactivity during the fabrication of sintered polymeric scaffolds. *Biomed Mater* 2014; 9: 025015.
- [36] Liu K-Z, Dixon IMC, Mantsch HH. Distribution of collagen deposition in cardiomyopathic hamster hearts determined by infrared microscopy. *Cardiovasc Pathol* 1999; 8: 41–47.
- [37] Segtnan VH, Isaksson T. Temperature, sample and time dependent structural characteristics of gelatine gels studied by near infrared spectroscopy. *Food Hydrocoll* 2004; 18: 1-11.
- [38] Liu K, Jackson M, Sowa MG, et al. Modification of the extracellular matrix following myocardial infarction monitored by FTIR spectroscopy. *Biochim Biophys Acta* 1996; 1315: 73-77.
- [39] Rosellini E, Zhang YS, Migliori B, et al. Protein/Polysaccharide-based Scaffolds Mimicking Native Extracellular Matrix for Cardiac Tissue Engineering Applications. *J Biomed Mater Res A* 2018; 106A: 769-781.

Figure Legend

Figure 1: SEM micrographs of Gel/GE microspheres, acquired at different magnifications: (a, b) unloaded particles; (c, d) particles loaded with IGF-1 by method A (loading after cross-linking); (e, f) particles loaded with IGF-1 by method B (loading during cross-linking). (g-h) Histograms showing size dispersion for dry and swollen microspheres, respectively. For both samples, the size range was divided in bins of 10 μm each.

Figure 2: (a) Chemical map of unloaded microspheres; (b) Chemical map in function of Gel amide II, for unloaded microspheres; (c) Chemical map in function of Amide II absorption peak of IGF-1, for microspheres loaded by method A; (d) Second derivative spectra acquired from the chemical map in (c), in the inner core and on the surface of the loaded microsphere. Gel and IGF-1 absorption peaks are indicated by arrows; (e) Chemical map in function of Amide II absorption peak of IGF-1, for microspheres loaded by method B; (f) Second derivative spectra acquired from the chemical map in (e), in the inner core and on the surface of the loaded microsphere. Gel and IGF-1 absorption peaks are indicated by arrows.

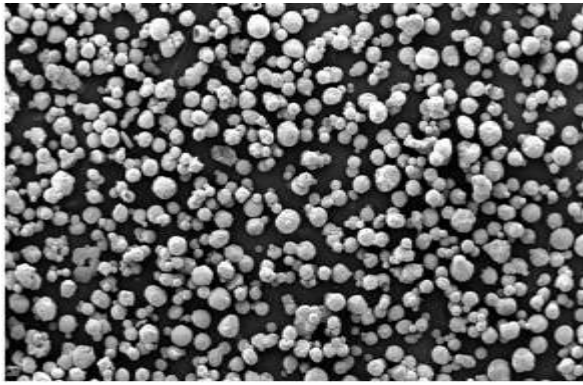
Figure 3: Release of IGF-1 from Gel/GE microspheres, loaded by adsorption after cross-linking (method A) or during cross-linking (method B).

Figure 4: Image merged from phase contrast and fluorescence microscopy illustrating the green fluorescence of cells seeded on microspheres functionalized with IGF-1 after 48h of culture in static conditions. Arrowhead indicates an example of cell laying over a microsphere. Scale bar = 200 μm .

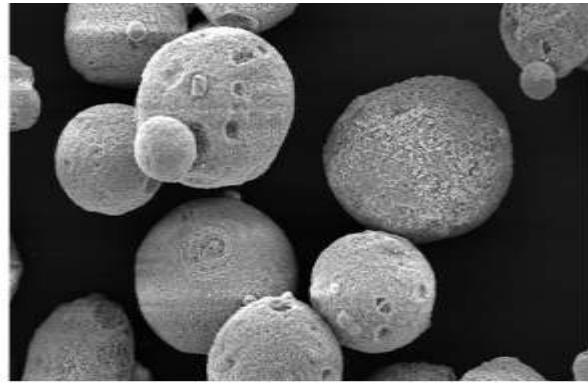
Figure 5: (a, b) Images merged from phase contrast and fluorescence microscopy showing Gel/GE microspheres with CPCs after 24h of dynamic suspension culture within the bioreactor. GFP^{pos} CPCs (green fluorescence) adhered to microspheres (a) or were located at the interface of two or more microspheres (b). Scale bars = 50 μm ; (c-f) Images merged from phase contrast and fluorescence microscopy showing CPCs and Gel/GE microspheres after 5 days of static cultures following dynamic suspension in bioreactor. GFP^{pos} CPCs (green fluorescence) still adhered to the surface, at times connecting multiple microspheres (white asterisk). Scale bars = 100 μm .

Figure 6: (a) Immunohistochemical detection within the rat myocardium of GFP^{pos} CPCs 4 days after injection of cells seeded on IGF-1 functionalized Gel/GE microspheres. Blue fluorescence corresponds to DAPI staining of nuclei (Scale bar = 500µm). (b) Bar graph showing the quantification of CPC homing to the damaged myocardium after their injection with Gel/GE microspheres (Gel/GE). **p<0.01 vs Gel/GE 4 Days; #p<0.05 vs Gel/GE+IGF-1 4 Days.

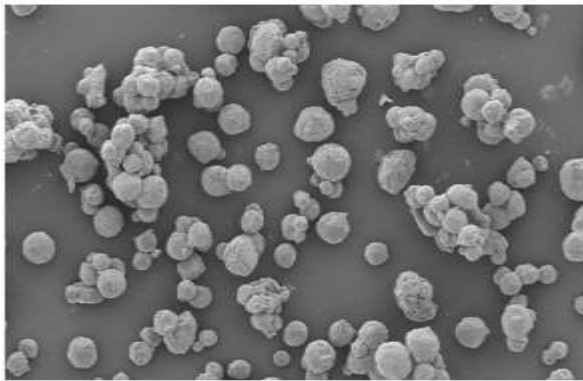
Figure 7: (a) Medium spectrum acquired from the chemical map of native rat myocardium; (b) Second derivative spectrum for native rat myocardium; (c) Medium spectrum acquired from the chemical map of explant sample; (d) Second derivative spectrum for explant sample.



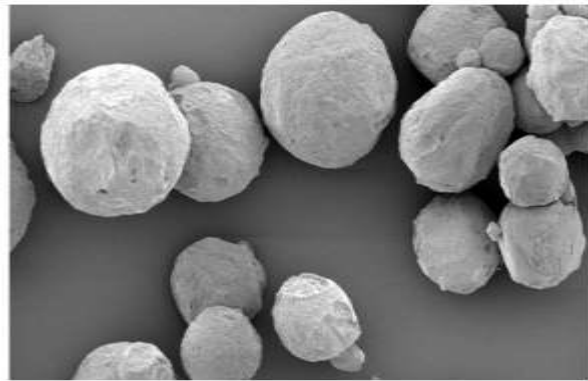
a) x 50 _____ 500 μm



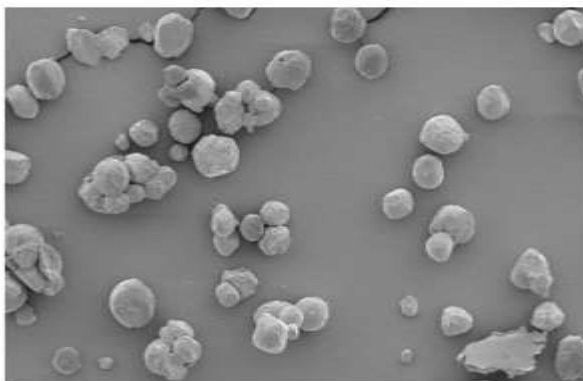
b) x 500 _____ 50 μm



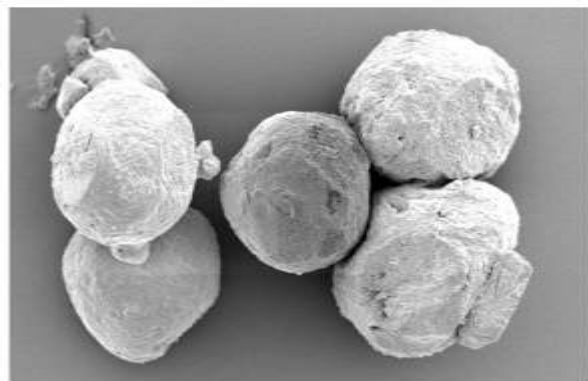
c) x 100 _____ 100 μm



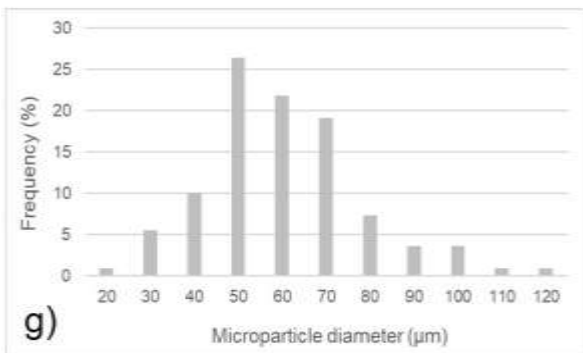
d) x 400 _____ 50 μm



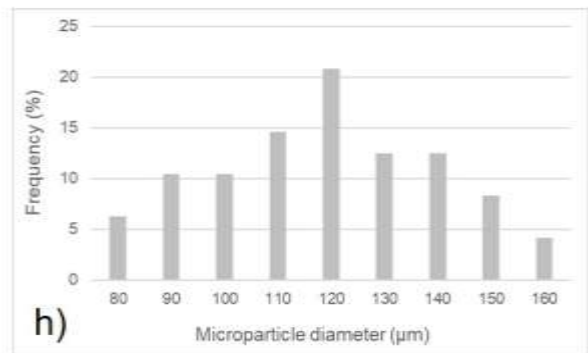
e) x 100 _____ 100 μm



f) x 600 _____ 20 μm



g)



h)

Figure 1

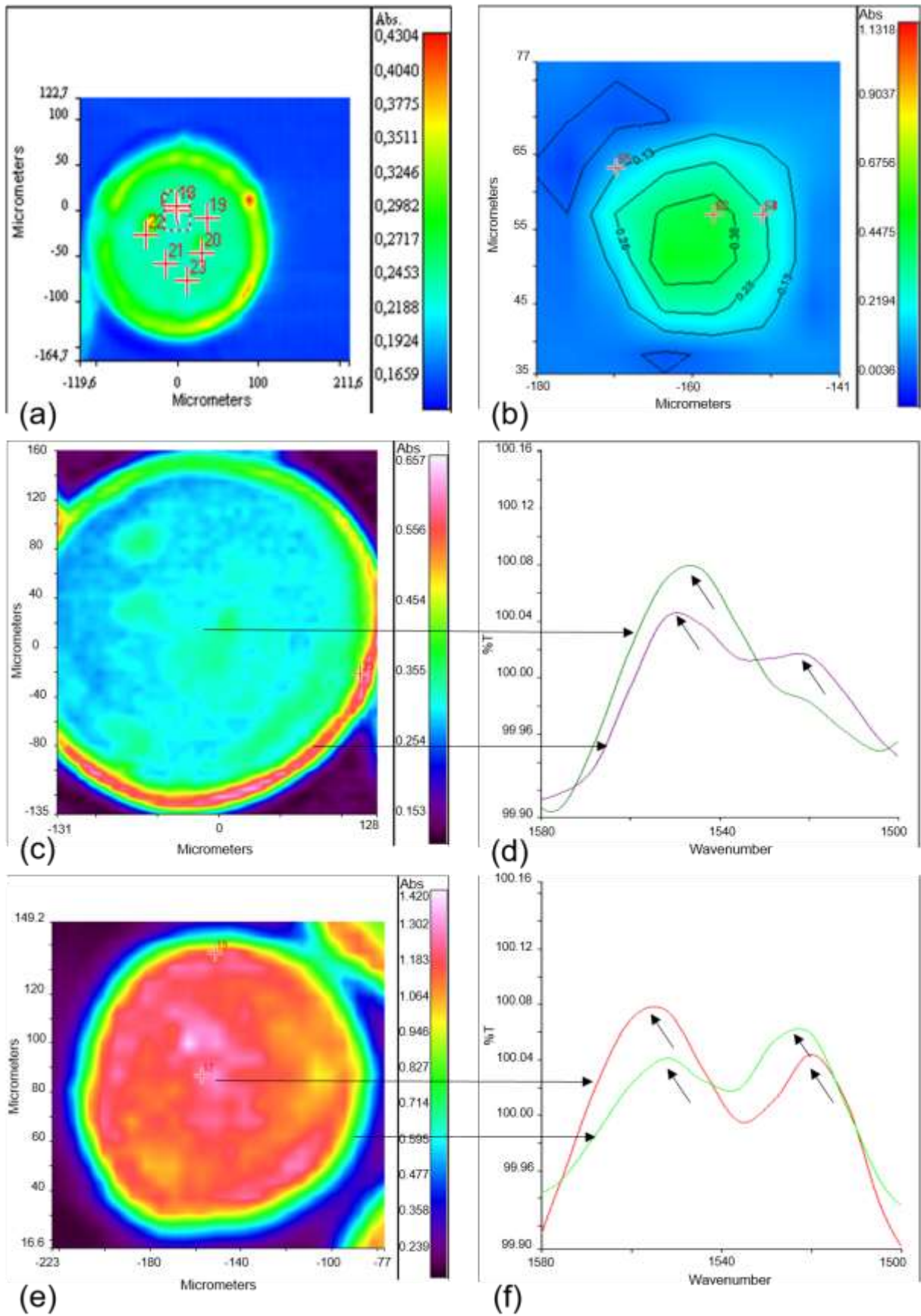


Figure 2

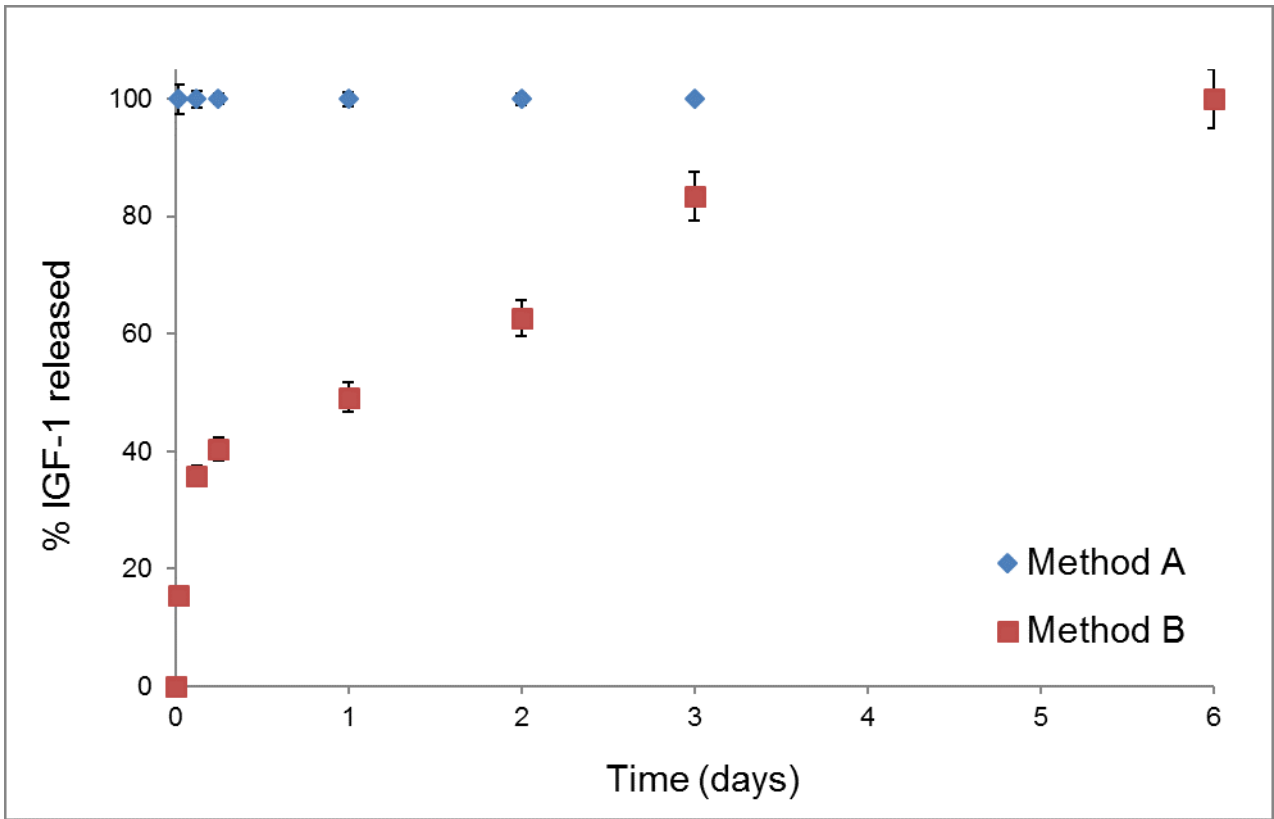


Figure 3

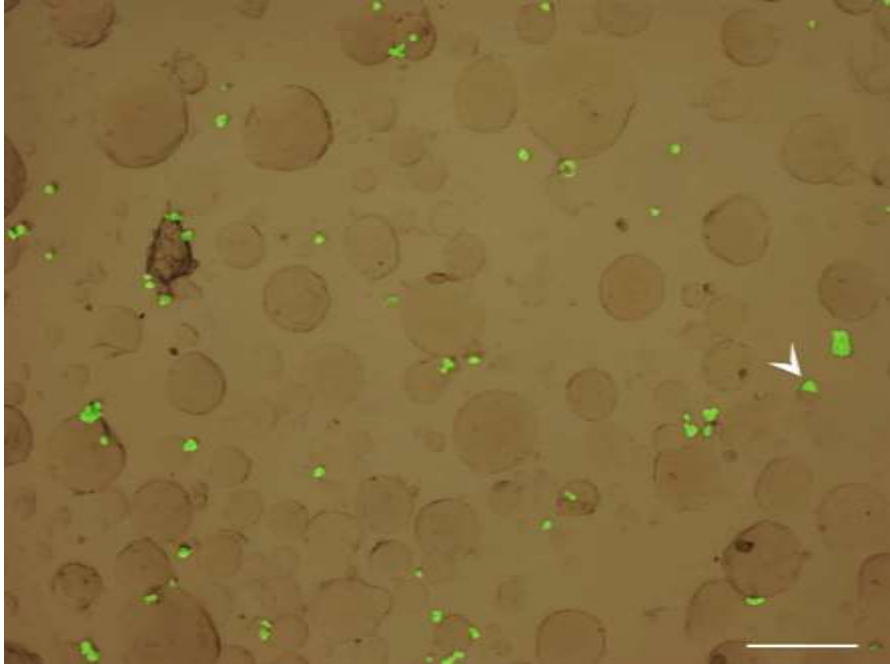


Figure 4

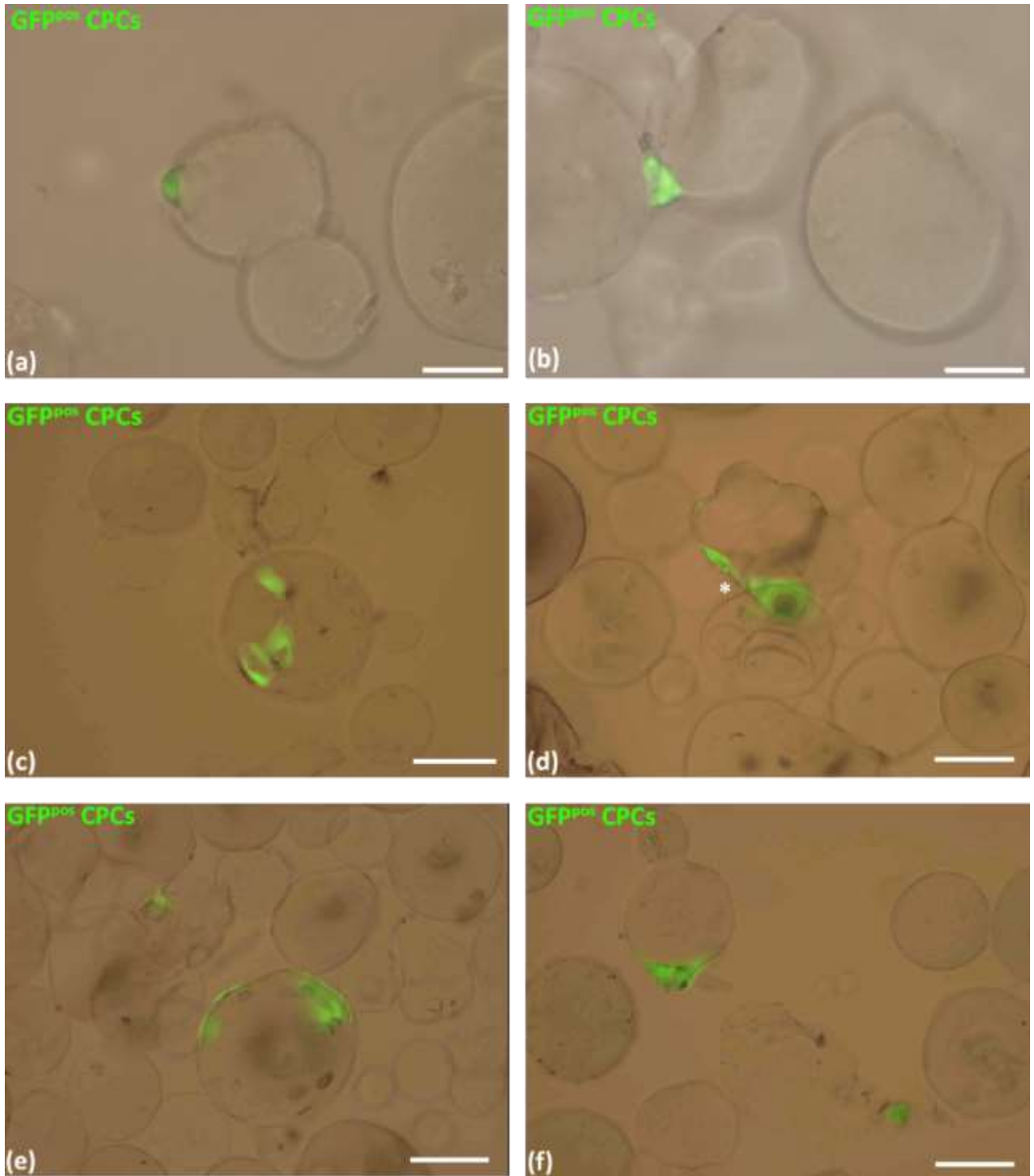


Figure 5

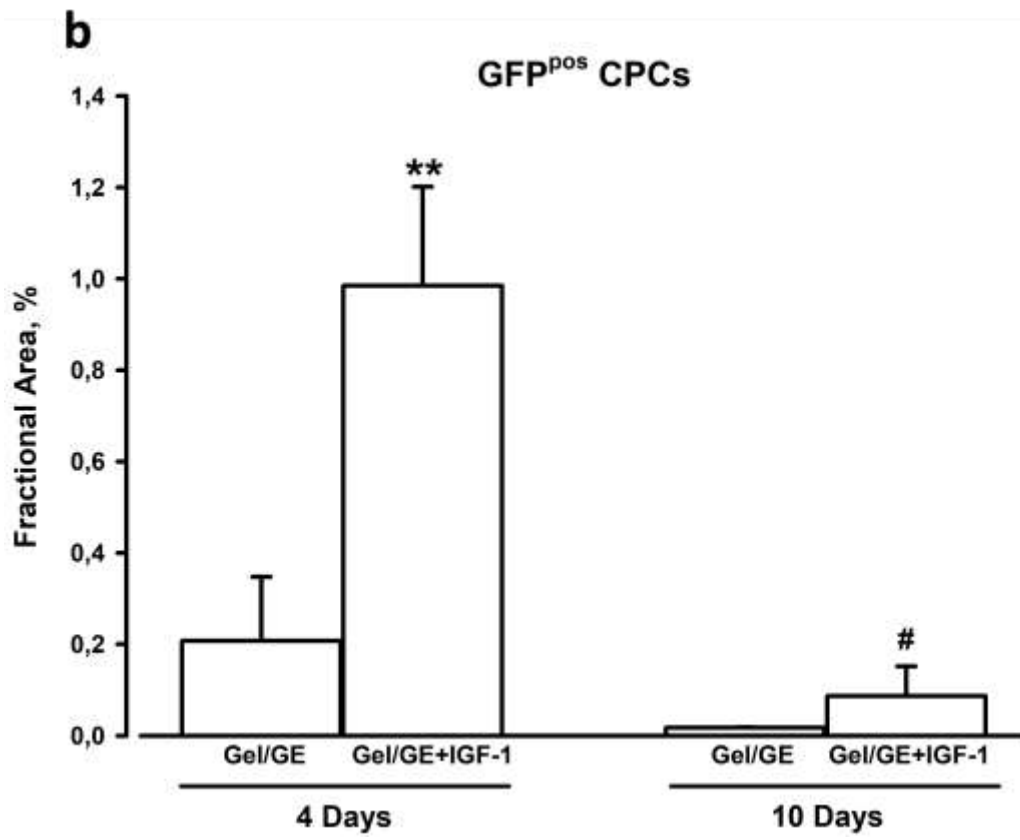
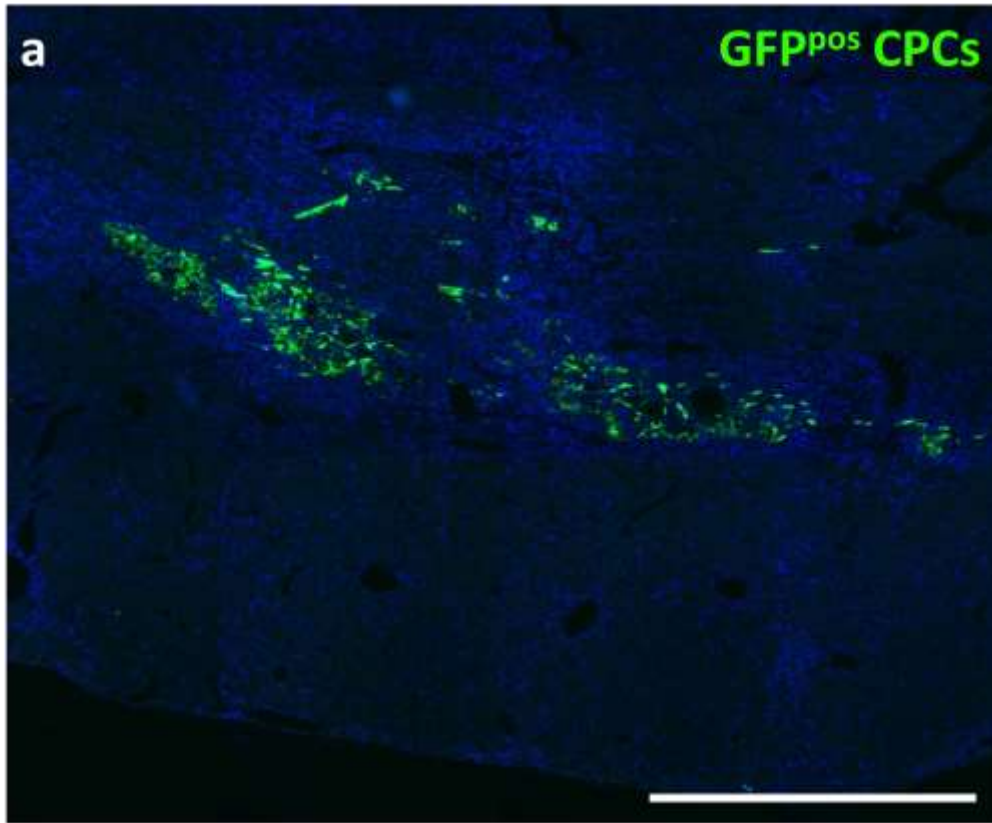


Figure 6

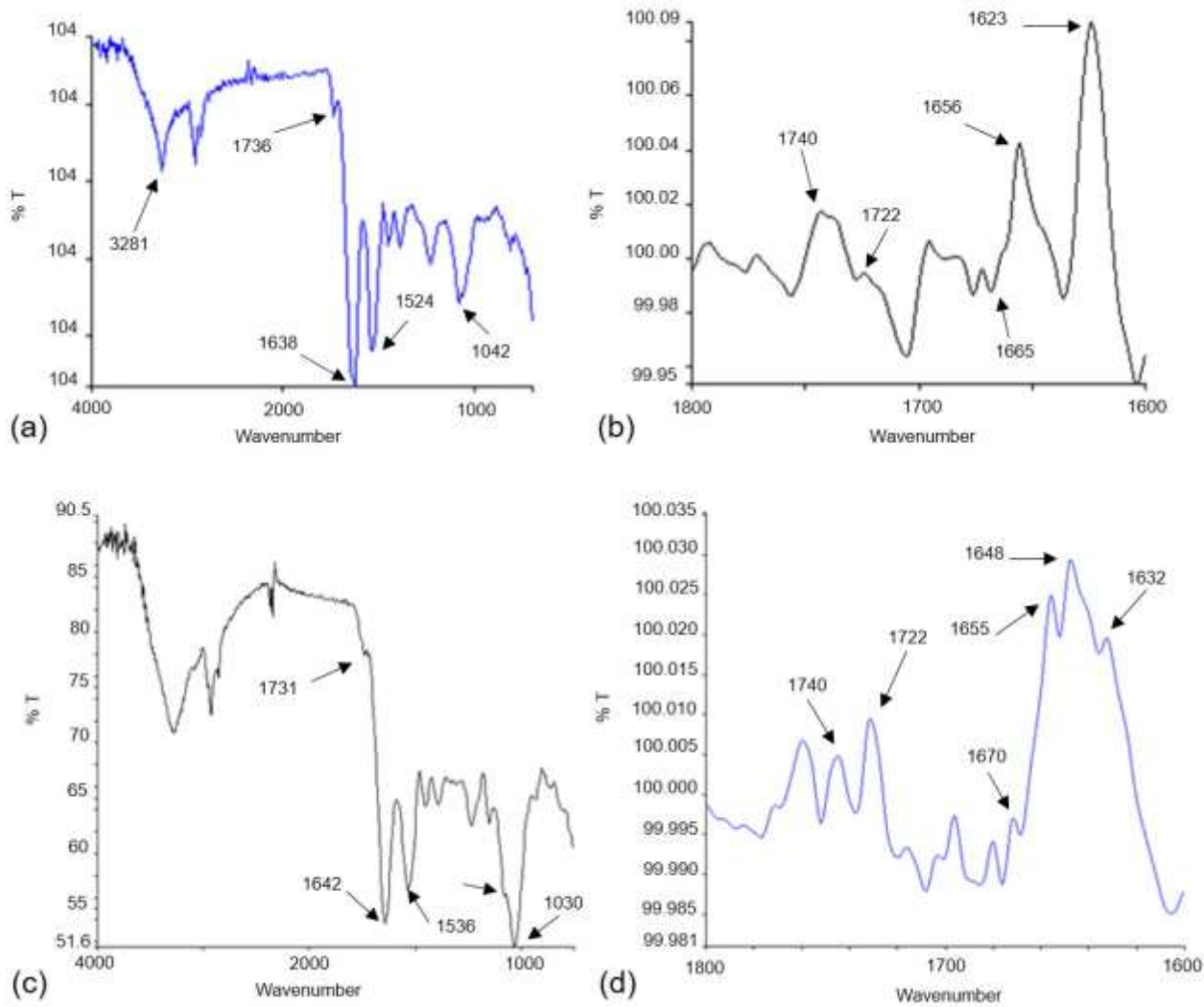


Figure 7